NEUROIMAGE 2, 221–229 (1995)

Activation of Prefrontal Cortex in Children during a Nonspatial Working Memory Task with Functional MRI

B. J. CASEY,* JONATHAN D. COHEN,*,† PETER JEZZARD,‡ ROBERT TURNER,§ DOUGLAS C. NOLL,¶,‖ ROLF J. TRAINOR,* JAY GIEDD,** DEBRA KAYSEN,** LUCY HERTZ-PANNIER†† AND JUDITH L. RAPOPORT**

*Departments of *Psychiatry and ¶Radiology, University of Pittsburgh, Pittsburgh, Pennsylvania 15213; †Psychology Department and ‖Department of Computer Science, Carnegie Mellon University, Pittsburgh, Pennsylvania 15213; ‡Cardiac Energetics, National Heart, Lung, and Blood Institute, **Child Psychiatry Branch, National Institute of Mental Health, and ††Diagnostic Radiology, National Institutes of Health, Bethesda, Maryland; and §RCS Biophysics Unit, Institute of Child Health, London, England*

Received March 24, 1995

Functional magnetic resonance imaging (fMRI) was used to examine the pattern of activity of prefrontal cortex in prepubertal children during performance of a nonspatial working memory task. The children observed sequences of letters and responded whenever a letter repeated with exactly one nonidentical letter intervening. In a comparison task, subjects monitored similar sequences of letters for any occurrence of a single, prespecified target letter. Location of activation closely approximated that observed in a recent fMRI study with adults using exactly the same task. Activation of the inferior and middle frontal gyri was reliably observed within individual subjects during performance of the working memory task relative to the comparison task. Activation increased and decreased with a time course that was highly consistent with the task manipulations and correlated with behavioral performance. To our knowledge, this study is one of the first to demonstrate the applicability of fMRI to a normative developmental population. Issues of age dependence of the hemodynamic responses of fMRI are discussed.

INTRODUCTION

Disturbances in cognitive processes involved in behavioral inhibition and memory have been implicated in a number of childhood onset psychiatric illnesses including attention deficit hyperactive disorder (ADHD), obsessive compulsive disorder (OCD), and schizophrenia (Trommer *et al.,* 1991; Harvey, 1987; Goldman-Rakic, 1991). Proposed anatomic regions that are responsible for these processes are regions within the prefrontal cortex (Mesalum, 1985; Fuster, 1989; Goldman-Rakic, 1987). Likewise, a number of these psychiatric disorders have demonstrated abnormal metabolism in the prefrontal cortex. For example, hypometabolism of the mesial prefrontal cortex and anterior cingulate has been observed in depressed patients (George *et al.,* 1993), while hypermetabolic activity has been observed in the anterior cingulate and orbitofrontal cortex in obsessive compulsive patients (Swedo *et al.,* 1989). Clearly, frontal circuits appear to be affected in these developmental psychiatric disorders.

To understand the role of the prefrontal cortex in these developmental psychiatric illnesses, it is important to understand the normal development of prefrontal circuitry. The prefrontal cortex continues to develop well after birth as do other cortical regions. This development consists of a series of biological changes marked by an initial abundance of cells, branches, and connections, with later pruning or cell death. This process reflects a developmental course of sculpting and fine tuning.

Evidence of pruning and reorganization of the prefrontal cortex during childhood comes from a study by Huttenlocher (1979), who reported changes in synaptic density in the frontal cortex over the life span. Huttenlocher observed increases in synaptic density well above adult levels over the first year of life with a steady decline in synaptic density over the next 16 years, which was then maintained at adult levels until approximately 72 years, at which time a slight decrease in a small sample of 74 to 90 year old brains was observed. Thus, even "at age seven when the child's brain is almost identical in size and weight to that of the adult, average synaptic density in frontal cortex is roughly 1.4 times that of the adult value" (Chugani *et al.,* 1987). More recently, Huttenlocher *et al.* (1982) published further data of synaptic density in the visual cortex. The peak in density and its time course were slightly earlier than observed in the prefrontal cortex. The peak in density occurred at roughly 8 months and adult levels were observed at 11 years. These results

1053-8119/95 $12.00

suggest that sensory cortex matures earlier than frontal and association cortex.

The time course of initial overproduction and subsequent elimination of synapses known to occur in the developing brain matches local cerebral metabolic rates for glucose (Chugani *et al.,* 1987). A 2-deoxy-2[18F]flouro-D-glucose (FDG) study of children aged 5 days to 15 years who suffered transient neurological events not significantly affecting normal neurodevelopment revealed a rapid increase in local cerebral metabolic rates for glucose from birth (5 days) to 3 to 4 years and then maintained until 9 years of age when they began to decline and reach adult rates by the end of the second decade. Similarly, Kennedy and Sokolov (1957) demonstrated that the average global cerebral blood flow in children (ages 3–11 years) was close to 2 times that of normal young adults and the average cerebral oxygen utilization was approximately 1.3 times that of adults. These findings are consistent with the overabundance of dendritic processes and synapses in childhood, relative to that in adulthood. Thus, the large surface area of processes may lead to higher metabolic rates for maintenance of membrane potential. As the synaptic density decreases, so does metabolic rate. An alternative, but not orthogonal, explanation is that a higher metabolic rate corresponds with excessive fuel expenditure by oligodendroglia during myelination. Incomplete myelination may therefore result in poorer conduction efficiency and thus greater energy expenditure. Regardless, the high metabolic rates observed during rest in children may suggest that as these rates decline along with synaptic density, the signal-to-noise in active tissue increases.

The examination of the functional integrity of prefrontal cortex and its development requires a methodology for examining brain state changes in developmental populations. Until recently, such structure–function relations have been limited to adult populations due to the inherent reliance of neuroimaging methods on radioactive isotopes. Thus, developmental psychiatric disorders have traditionally been studied in adulthood, well after onset of the symptoms. A noninvasive neuroimaging technique, functional magnetic resonance imaging (fMRI), has been developed that can be used to examine brain state changes (Ogawa *et al.,* 1990; Turner *et al.,* 1991; Kwong *et al.,* 1992). This technique is based on the observation that hemoglobin becomes highly paramagnetic in its deoxygenated state. Thus, deoxygenated hemoglobin can be used as a naturally occurring contrast agent, with highly oxygenated areas producing a larger magnetic resonance (MR) signal than less well oxygenated regions.

The current study examines activation of prefrontal cortex in children using this technique—functional MRI. It is our hope to ultimately determine the utility of this method not only in the study of normal development of higher cognitive processes, but also in the study of developmental psychiatric disorders with prefrontal dysfunction. This study uses a nonspatial working memory task to examine brain state changes in prefrontal cortex of children. We have used this exact task successfully to demonstrate frontal activation in adults using fMRI (Cohen *et al.,* 1994).

METHODS

Cognitive Tasks

Six right-handed subjects were studied, three males and three females, ranging in age from 9 to 11 years. Subjects were scanned while they performed a working memory task and a control task. In both tasks, subjects observed random sequences of letters appearing one at a time in the center of a visual display and were instructed to respond by pressing a button on a handheld fiber optic response box whenever a target appeared (see below). Stimuli were presented for 500 ms, with an interstimulus interval of 1000 ms. Stimulus presentation was controlled by a Macintosh IIci computer and rear-projection screen using a high-luminance overhead projector and an LCD panel connected to the computer (for details see Cohen *et al.,* 1993).

In the control task, a target was any occurrence of the letter "X". In the memory task, targets were any letter that repeated with exactly one intervening nonidentical letter (e.g., A–F–A, but not A–A or A–Q–G–A). Target frequency (1/7) and the frequency of repeated letters were matched in the two tasks. Thus, the only differences between the tasks were the appearance of the letter "X" in the control but not the memory task and the instructions given to subjects. Both the control and the memory tasks required that subjects monitor sequences of letters presented visually one at a time, encode each letter, evaluate its identity, and respond to a target by pressing a button. However, the memory task had the additional requirement that the subject keep in mind both the identity and the order of the two previous letters and continuously update this mental record as the sequence progressed. These operations are central to the concept of working memory, as it has been defined in cognitive psychology (Baddeley, 1986), and our task is very similar to others that have been used to study working memory (e.g., Gevins and Cutillo, 1993).

Scanning Procedures

Scans were acquired at eight contiguous coronal slice locations in the prefrontal cortex of the six volunteer subjects. Functional images were acquired using multislice, echo planar imaging techniques on a 1.5T GE Signa whole body scanner (Turner *et al.,* 1991). Two 5-in. receive-only surface coils, mounted on each side of

the head, were used to maximize signal-to-noise. Functional scans were 5 mm thick, with 64 × 64 pixels (3.1 × 3.1 mm) in plane, acquired at eight contiguous locations with the center of the posterior-most slice aligned with the posterior margin of the genu of the corpus callosum. Structural images were obtained at these locations prior to functional scanning, using a standard T1-weighted sequence. Functional images were acquired using a gradient-echo echo planar sequence with a TR of 6000 ms, a gradient echo TE of 40 ms, a flip angle of 90, and a field of view of 20 cm. A set of images from all eight slice locations was obtained every 6 s. Twenty sets were obtained during each 120-s task block, for two blocks in each task, providing a total of 40 scans at each slice location in each task. The conditions were run in an ABBA sequence to control for systematic changes over time (Bench *et al.,* 1993), and each block of scans began approximately 6 s after task onset to allow time for a change in the MR response. Previous studies suggest that the maximum MR response is typically within 3–6 s of task onset (Belliveau *et al.,* 1992; Blamire *et al.,* 1993; Frahm *et al.,* 1993).

ANALYSIS

Image processing. Each set of 80 functional images acquired at a given plane location was scaled to a common mean (to reduce the effects of global signal drift or other forms of scanner instability) and registered in-plane using a simple sum squared error reduction algorithm. Mean normalization was performed as follows: First, the mean pixel value was computed for one image in the set, to act as a reference. The same computation was then performed for each other image in the set, and the value of each pixel in a given image scaled by the ratio reference mean/image mean. Images were then registered to a reference image to control for movement during the scanning procedure using a modified version of Roger Woods' 3-D automated image registration (AIR) (Woods *et al.,* 1992). In-plane movement in rotation, and x and y directions were plotted for each subject for each image location and time point. Movement did not correlate with the experimental manipulation, but rather appeared to increase as a function of time in the scanner. Average absolute movement for the entire study was 0.35° in rotation, 0.34 mm in the x direction, and 0.47 mm in the y direction.

Statistical subtractions and anatomic localization. Statistical subtraction procedures were applied to the functional scans (memory − control) for each subject separately. Areas of significant activation at each scan location were identified by performing pixel-wise t tests between images acquired during the control and memory tasks using a split-halves method, as follows. For each slice location, the first 20 scans acquired during the control task were compared with the first 20 acquired during the memory task using a standard pixel-wise t test. The same procedure was applied to the second set of 20 images under each condition. Areas were then identified that had t values of 3.56 or greater ($P < 0.001$, one-tailed) in both comparisons. This procedure has been used successfully in a study of prefrontal cortex (Cohen *et al.,* 1994) and visual cortex as well (Schneider *et al.,* 1994).

Because any image consists of a large number of pixels, the probability of a false positive can become quite large, unless some adjustment for multiple comparisons is made. Most frequently, Bonferroni adjustments are made which would be equal to a P value of 0.00001 ($0.05/(64)^2 = 0.05/4096 = 0.000012$). Our significance levels for the split-halves statistic approximate this value (i.e., $P < 0.001)^2 = 0.000001$ approximated estimate). Because the current study had a spatial resolution roughly three times coarser than that of the adult study by Cohen and colleagues using spiral scanning (1994), we chose not to eliminate smaller areas of activation in children with contiguity threshold analysis, but instead to set our significance level at a more conservative level.

Areas (in number of pixels) of activation were computed, as well as their mean and peak t values. These regions were then overlaid on the corresponding structural images, to identify their exact locations, and assigned to one of the five anatomic structure categories listed in Table 1. Assignment of regions of activity to structures was performed independently by two raters, using a standard magnetic resonance imaging brain atlas as a reference (Duvernoy, 1991) and surface renderings of the frontal gyri. Interrater reliability on this procedure was greater than 0.9, and a consensus rating was performed on those areas for which the individual ratings did not agree. Only regions that did not lay over vessels identifiable in the structural images were categorized. The regions that satisfied this criterion were presumed to be associated with capillaries or sufficiently small vessels as to reflect effects localized to the structure with which they were identified. In some images, there were also areas of significant differences along the rim of the cortex, usually unilaterally; these were believed to be related to motion artifact and were excluded from analysis (as per Kim *et al.,* 1993).

Quantitative analysis of the anatomic distribution. This was performed by conducting analyses of variance (across subjects) examining the number, size, and significance of regions of activation within the anatomic structures and hemispheres listed in Table 1.

Time series. Finally, the mean MR signal for each anatomic structure was plotted as a function of time. Specifically, plots were generated by first computing the mean value of the pixels associated with each region of activity at each time point (i.e., scan) for each subject. These means were then averaged for all of the

TABLE 1

Statistics for Areas of Activation for Each Region of Interest by Hemisphere across Subjects

Regions of interest	Subjects	Location (x,y,z)	N	Area (mm^2)	% diff	Mean t	Peak t
Superior frontal	—	—	—	—	—	—	—
	3	11, 19, 35 (R)	3	9	5.7	5.9	6.7
Middle frontal	3	−44, 38, 19 (L)	13	60	3.8	6.5	9.3
	5	33, 34, 26 (R)	14	48	4.3	6.9	9.7
Inferior frontal	4	−41, 30, 12 (L)	27	121	3.1	6.2	7.7
	4	43, 27, 7 (R)	19	74	4.8	6.8	9.3
Anterior cingulate	1	−7, 29, 12 (L)	2	23	2.2	6.0	8.4
	3	6, 32, −12 (R)	7	11	4.2	5.6	7.0
Orbital gyrus	1	−25, 37, −16 (L)	2	43	5.0	6.1	8.3
	1	14, 38, −15 (R)	8	93	5.7	6.8	8.8

Note. This table reports statistics for areas of activation in the superior frontal gyrus, middle frontal gyrus, inferior frontal gyrus, anterior cingulate, and orbital gyri. For each structure the following data are reported: the number of subjects showing activation in that structure in the left and right hemispheres; the mean of the x (left–right), y (anterior–posterior), and z (superior–inferior) coordinates for areas of activation relative to the anterior commissure (which was identified in a midsagittal image for the corresponding subject); the total number of activated areas identified across subjects (N); total area of activation, computed first within subjects and then averaged across subjects; percentage change in signal intensity averaged across subjects; mean t values for activated area averaged across subjects; peak t values for activated area averaged across subjects. Averages are across only those subjects showing activation in the corresponding structure.

regions within each anatomic category, to generate a mean value for regions of activity within each structure at that time point for each subject. These were then reexpressed as a percentage difference from the mean of such values across all time points (i.e., all 80 scans). Finally, the percentage difference values at each time point for each structure were averaged across subjects and plotted as a function of time.

RESULTS

Reliable activation was observed in the inferior and middle frontal gyri. While some subjects showed greater activation than others, five of six subjects showed significant activation in both of these two structures and four showed bilateral activation of one or both of these structures (refer to Table 1 and Fig. 1). The majority of activated areas in the inferior and middle frontal gyri fell within Brodmann's area 46 and 10, respectively (Talairach and Tournoux, 1988). In addition, half of the subjects showed activation in the cingulate and orbital frontal gyri (Brodmann's areas 32 and 11, respectively). An ANOVA with structure and hemisphere as factors and number of activated areas as the dependent measure showed only a significant main effect of structure ($F = 4.92$, $P < 0.006$). Posthoc comparisons (pairwise t tests of all structures, using a Tukey–Kramer correction for multiple comparisons) were conducted to explore the main effect of structure. There were a significantly greater number of activated areas observed in the inferior frontal gyri ($P < 0.05$) than in all other structures, except for the middle frontal gyri.

We plotted the data by individual block to assess reliability across the study. Figure 2 depicts the percentage difference in signal across scans and averaged across subjects for the middle and inferior frontal gyrus. Both of these regions were reliably activated across subjects. As is demonstrated for the middle and inferior frontal gyrus across six prepubertal children, the change in percentage difference corresponds nicely with the experimental manipulation across the four blocks of 20 images.

We further analyzed the data in separate halves to assess intrasubject reliability. This split-halves methodology has been described in the past as a method for determining test–retest reliability in the statistical literature (Snedecor and Cochran, 1980) and has been effectively applied to fMRI data (Cohen *et al.*, 1994; Schneider *et al.*, 1994). Figure 3 illustrates this reliability in a representative coronal slice of a 10-year-old female. Figure 3A depicts the results of the split-halves methodology overlaid onto a T1-weighted image (i.e., intersection of active areas in both sets of pixel-wise t test analyses on each half of the data.) Figures 3B and 3C depict the two t maps representing the analysis from each respective half of the data. Note that the same regions are activated across halves.

To further illustrate the utility of this statistical analyses, Figure 4 depicts an overlay of a simple t map

FIG. 1. Orthogonally projected regions of activation onto frontal views of surface renderings created from 3-D volumetric MR data sets of each subject's brain.

FIG. 3. (A) Activation based on split-halves t tests overlaid onto a T1-weighted coronal image. (B and C) The two t maps representing each half of these data.

FIG. 4. (A) An overlay of activation on a T1-weighted image based on pixel-wise t tests. (B) An overlay of activation on a T1-weighted image based on pixel-wise t tests using split halves. (C) An overlay of activation (or lack of it) on a T1-weighted image based on pixel-wise t tests comparing the first and second halves of the control data.

	Peak *t*
	—
	6.7
	9.3
	9.7
	7.7
	9.3
	8.4
	7.0
	8.3
	8.8

l gyrus, anterior
n that structure
ates for areas of
he total number
across subjects;
eak *t* values for
tructure.

r frontal gy-
ly activated
e middle and
tal children,
ponds nicely
oss the four

ate halves to
halves meth-
a method for
tatistical lit-
nd has been
et al., 1994;
tes this reli-
a 10-year-old
split-halves
image (i.e.,
pixel-wise *t*
ures 3B and
the analysis
ote that the

s statistical
simple *t* map

ion onto frontal
netric MR data

ts overlaid onto
ps representing

veighted image
ation on a T1-
t halves. (C) An
image based on
es of the control

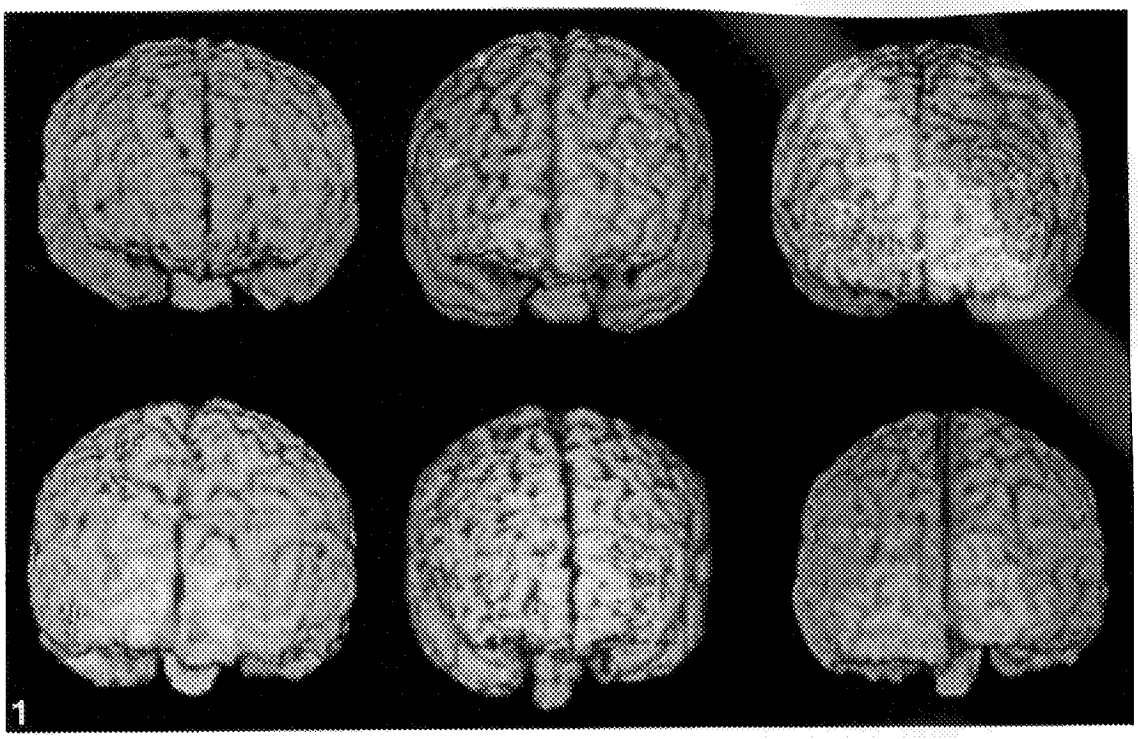

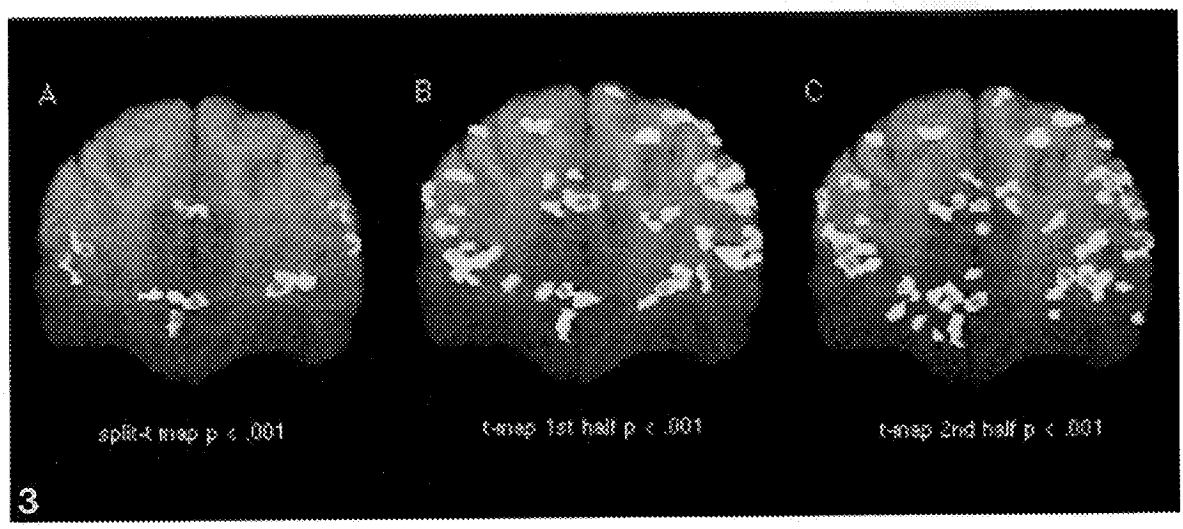

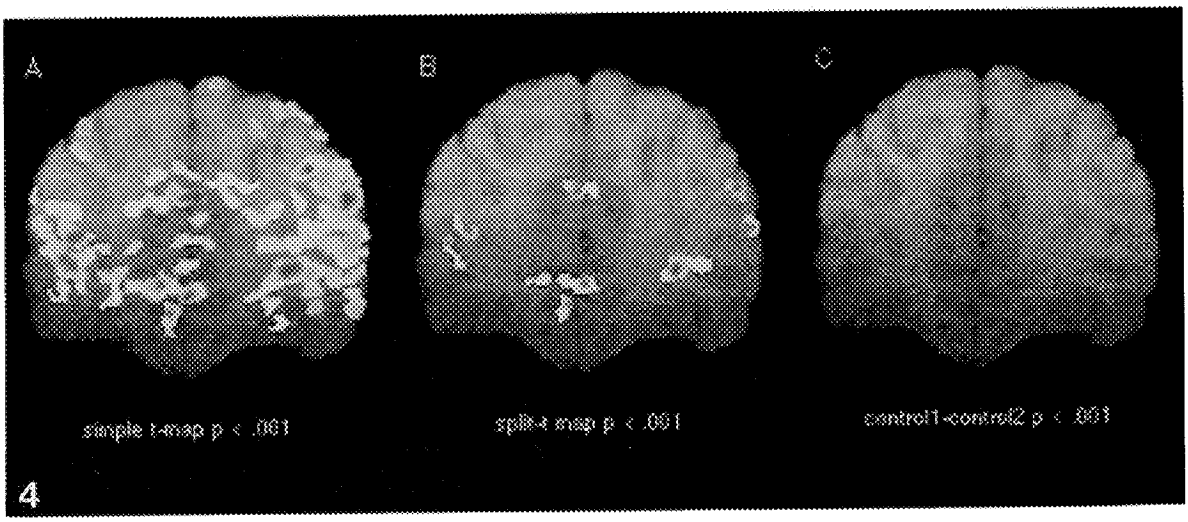

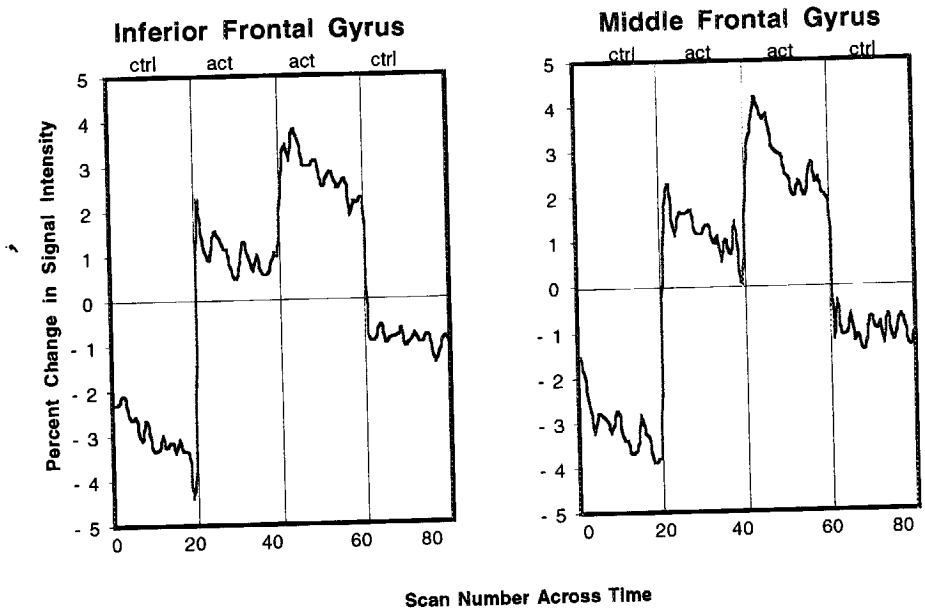

FIG. 2. Percentage difference in MR signal across time averaged across subjects for the middle and inferior frontal gyri for two blocks of 20 images per task condition.

without using the split-halves analysis in Fig. 4A and an overlay of a split-halves t-map in Fig. 4B. The split-halves *t* map reveals activation over the expected regions of interest. Figure 4C reflects an analysis of the control data comparing the first half against the second. No false positives were detected, further indicating the strength of this methodology.

Developmental Differences

Finally, we examined developmental trends across the ages of 9 and 11 years by comparing the magnitude of the change in MR signal across subjects. This measure was selected because we thought it may be correlated with previous reported local cerebral metabolic rates for glucose, blood flow, and oxygen utilization in children. Table 2 reflects percentage difference in signal intensity for areas of activation in two of the most reliable brain regions of activation: the middle and inferior frontal gyri. The percentage difference in signal intensity increases across the ages of 9 to 11 years in both structures ($r = 0.82$, $P < 0.005$). Note that the youngest subject failed to show activation in these regions.

TABLE 2

Percentage Difference in Signal Intensity for Area of Activation in the Inferior Frontal Gyri and the Middle Frontal Gyri for Six Children between the Ages of 9 and 11 Years

	Subject					
	1	2	3	4	5	6
Age in months	115	118	120	131	133	139
Gender	F	M	F	F	M	M
IFG						
% diff. in MR signal	*	2.6	2.5	3.5	5.4	4.6
MFG						
% diff. in MR signal	*	3.2	3.8	5.4	4.7	5.5

* Areas of activation did not reach significance for this subject.

DISCUSSION

To our knowledge, this is the first study to examine development in higher cognitive function using fMRI. Our results replicate those observed in adults as reported by Cohen *et al.* (1994). Both studies revealed activation in the middle and inferior frontal gyri within individual subjects during performance of a working memory task relative to the comparison task. The results of this study indicate that it is possible to use fMRI to study the activity of prefrontal cortex in children and they corroborate findings from PET studies that areas of prefrontal cortex are activated during the performance of a task that relies on working memory.

Developmental Effects

The similarities in overall location of activation across the two studies are uncanny. The distribution across regions was the same for both. The greatest amount of activation was observed in the inferior frontal gyrus, especially the left, followed by bilateral activation of the middle frontal gyrus. In addition, a small percentage of subjects showed activation in either the right or the left orbitofrontal, anterior cingulate, and/or superior frontal gyri. Again, distribution of activa-

tion across these regions was almost identical to the distribution observed in adults with more activation in the orbitofrontal cortex than in the anterior cingulate and the least activation in the superior frontal region.

Although identical locations of activation were observed across the two studies, there appeared to be smaller areas of activation distributed across these distinct areas of the prefrontal cortex in children relative to the adults. These differences may be attributed to differences in scanning parameters. The current study used echo planar imaging and had a spatial resolution roughly 3 times coarser than that of the adult study by Cohen and colleagues using spiral scanning. Alternatively, these results may reflect a more diffuse pattern of activity in children relative to that in adults. This interpretation is consistent with findings of another developmental functional MRI study of children with seizures (Hertz-Pannier *et al.,* 1994). According to this work, there was a prominence of diffuse activation in children relative to adults. The observed diffuseness of activation may reflect immature cortical reorganization (i.e., synaptic pruning and myelination) in children. However, a larger sample and age range are needed to further evaluate this explanation.

Developmental trends were assessed within this study by comparing the magnitude of the MR signal across subjects. Evidence of possible developmental differences as reflected in the magnitude of the MR signal (percentage difference in MR signal intensity) in children is depicted in Table 2. The percentage difference in signal intensity appears to increase across the ages of 9 to 11 years. This result may suggest that as local cerebral metabolic rate begins to decline and synaptic density continues to decrease, the signal-to-noise in active tissue increases. Alternatively, the younger subjects may be using different cognitive strategies to perform the task. These two explanations are not orthogonal. Younger subjects may have to rely on alternative cognitive strategies in performing the task due to less efficient synaptic connections (or greater synaptic density). Regardless, these results suggest the importance of establishing the normative developmental curve of the hemodynamic responses of fMRI before we can interpret fMRI results with developmental psychopathologies. However, with the current small sample size and age range this conclusion is only speculative.

Effect Size

In the current study, the magnitude of signal change ranged from 2 to 5% across areas (average = 4.3%). The magnitude of the signal change observed in adults (Cohen *et al.,* 1994) on this task ranged from 1.1 to 3.8% across areas (average of 2.0%). Hertz-Pannier reported a similar range of 1.5 to 3.5% in her study on language lateralization in children (1994). One factor which may have contributed to these magnitudes is that the working memory task we used required continuous maintenance and updating of letters in memory. This contrasts with tasks used in previous neuroimaging studies of working memory, which allowed subjects to "unload" working memory after each response (e.g., Paulesu *et al.,* 1993). The continuous demands placed on working memory in our task may be more similar to the conditions used to produce activation in sensory and motor areas, in which stimuli or motor activity are sustained continuously throughout each block. Alternatively, the spatial and temporal resolution of this methodology may provide a more sensitive measure of signal change.

Another explanation for this effect is that performance of this task may require greater working memory demands on children relative to adults. In a recent fMRI study (Braver *et al.,* 1995) of working memory in adults, monotonic increases in activation were observed as a function of increasing memory load. There is general consensus that working memory continues to develop throughout childhood and adolescence (Baddeley, 1986). For example, the number of items that can be maintained in memory systematically increases with age (Pascal-Leone, 1970). Whether this increase reflects an increase in memory capacity (Pascal-Leone, 1970) or the development of more efficient control processes or strategies (Case *et al.,* 1982) is largely debated. However, this cognitive development appears to parallel the development of prefrontal cortex across this period. Therefore another interpretation of our larger effect size may be that greater demands are placed on working memory in children with this task than on adults. This interpretation is consistent with our low mean accuracy of 77% in children relative to 90% or greater in the adult studies using the exact task (Cohen *et al.,* 1994; Braver *et al.,* 1995).

Laterality Effects

Although our study did not provide direct evidence for lateralization of activation, there were a greater number of activated areas and a greater average area of activation in square millimeters represented in the left hemisphere, especially in the inferior frontal gyrus (refer to Table 1). We may not have had the sensitivity to measure laterality effects given the asymmetries in MR signal across the two hemispheres associated with the use of two receive-only surface coils. Although important, laterality and volumetric measures of these data are therefore limited in interpretation due to the asymmetry in the dual surface coils used in this study. Any differences in these measures may be due to this technical limitation in our study and may not represent true differences across the 9- to 11-year-age range.

Sources of Artifact

As noted, in a small number of images we observed areas of artifact overlying the cortical rim, which we

attributed to task-related movements. This raises the possibility that other regions of "activation" may also have been related to movement. While this may be the case, we do not believe that these significantly influence our results, for several reasons. First, these areas were observed in only a subset of subjects (two), whereas regions of activation overlying the inferior and/or middle frontal gyri were observed consistently across subjects. Furthermore, it seems unlikely that movement could account for the specific regional distribution of activation observed in our study (significantly greater activation of inferior and middle frontal gyri compared to the superior frontal, orbital, and cingulate gyri). Finally, studies of sensory (Schneider *et al.,* 1993) and motor (Kim *et al.,* 1993) cortices have also revealed areas of activation at the rim of the cortex and have used similar procedures for eliminating them from analysis. These studies have produced results that conform extremely well to what is known about the functional anatomy of these regions from direct electrophysiological examination in nonhuman primates, and there does not appear to be any reason to believe that circumstances should be different in association cortex.

Another potential concern surrounds the possibility that areas of activation reflect changes in the oxygenation state of large draining vessels that may serve regions anatomically removed from the areas in which effects are observed. When using a method of neuroimaging that relies on hemodynamic changes to index neural activity, it is important to consider potential disparities between vascular and parenchymal sources of signal. The two most likely causes for signal changes in blood vessels are the blood oxygenation effect in veins draining an area of activation and the flow-related enhancement in both supply and draining vessels based on activity-related changes in flow. Both effects could potentially occur in vessels distal to the actual site of neural activity.

We have taken two approaches to guard against vessel-related changes. First, signal changes associated with vascular flow can be mitigated with the appropriate choice of pulse sequence parameters, similar to the way that imaging pulse sequences can be sensitized to flow. For example, a single-slice study using a short TR and moderate flip angle will be highly sensitized to flow-related changes (Dyun *et al.,* 1993; Frahm *et al.,* 1993), while longer TR pulse sequences (3 or more s) should have little flow sensitization. The pulse sequence parameters we used in this study (6-s TR and 90° flip angle) have very little flow sensitivity. Second, we excluded from analysis areas of activation that lay over vessels identifiable within the structural scan. Our reasoning was that by eliminating areas of activation associated with vessels large enough to be observed, remaining areas would most likely be associated with vessels small enough to be serving relatively local regions. This assumption seems warranted, relative to the spatial resolution at which we analyzed our data, which was at the level of cortical gyri. We should also note that the magnitudes of our effect sizes (2–5%) were in the range that others, using high field systems (Menon *et al.,* 1993), have reported for small vessels and capillaries (<6%) and not in the range reported for larger vessels (e.g., >6%).

In conclusion, our results demonstrate brain state changes in prefrontal cortex in a developmental population using fMRI. Specifically, we observed task-related changes of brain activity in normal children similar to those observed in adults while performing a nonspatial working memory task. These changes can be localized to specific anatomic structures and follow a time course that closely track changes in the behavioral task. They also show response characteristics that are very similar to those observed in adults (changes of 2–5%). Our findings imply a great utility of fMRI in the study of the development of cognitive function across this age range. Finally, this work suggests that the hemodynamic response of fMRI used to assess neural activity may be age dependent.

REFERENCES

Baddeley, A. D. 1986. *Working Memory.* Oxford Univ. Press, New York.

Baddeley, A. D. 1992. Working memory: The interface between memory and cognition. *J. Cognitive Neurosci.* **4**(3): 281–288.

Bandetti, P. A., Wong, E. C., Hinks, R.S., Tikofsky, R. S., and Hyde, J. S. 1992. Time course of EPI of human brain function during task activation. *Magn. Res. Med.* **25:** 390–397.

Belliveau, J. W., Kennedy, D. N., McKinstry, R. C., Buchbinder B. R., Weisskoff, R. M., Cohen, M. S., Vevea, J. M., Brady, T. J., and Rosen, B. R. 1992. Functional mapping of the human visual cortex by magnetic resonance image. *Science* **254:** 716–719.

Bench, C. J., Frith, C. D., Grasby, P. M., Friston, K. J., Paulesu, E., Frackowiak, R. S. J., and Dolan, R. J. 1993. Investigations of the functional anatomy of attention using the Stroop test. *Neuropsychologia* **31:** 907–922.

Blamire, A. M., Ogawa, S., Ugurbil, K., Rothman, D., McCarthy, G., Ellermann, J. M., Hyder, F., Rattner, Z., and Shulman, R. G. 1993. Dynamic magnetic resonance imaging of human brain activity during primary sensory stimulation. *Proc. Natl. Acad. Sci. USA* **89:** 11069–11073.

Braver, T., Cohen, J. D., Jonides, J., and Smith, E. E. 1995. Parametric changes in frontal activity during a non-spatial working memory task using functional MRI. *Proc. Cognitive Neurosci. Soc.* [Abstract].

Case, R., Kurland, M., and Goldberg, J. 1982. Operational efficiency and the growth of short term memory. *J. Exp. Child Psychol.* **33:** 386–404.

Chugani, H. T., Phelps, M. E., and Mazziotta, J. C. 1987. Positron emission tomography study of human brain functional development. *Ann. Neurol.* **22:** 487–497.

Cohen, J. D., Noll, D. C., and Schneider, W. 1993. Functional magnetic resonance imaging: Overview and methods for psychological research. *Behav. Res. Methods, Instruments, Computers* **25**(2): 101–113.

Cohen, J. D., Forman, S. D., Braver, T. S., Casey, B. J., Servan-

Schreiber, D., and Noll, D. C. 1994. Activation of the prefrontal cortex in a nonspatial working memory task with functional MRI. *Hum. Brain Mapping* **1:** 293–304.

Duvernoy, H. M. 1991. *The Human Brain. Surface, Three-Dimensional Sectional Anatomy and MRI.* Springer-Verlag, New York.

Dyun, J. F., Moonen, C. T. W., DeBoer, R. W., Iperen, G. W., and Luyten, P. R. 1993. In-flow versus deoxyhemoglobin effects in BOLD fMRI using gradient echo at 1.5 T. In *The 12th Annual Scientific Meeting of the Society of Magnetic Resonance in New York.*

Frahm, J., Merboldt, K. D., and Hanicke, W. 1993. Functional MRI of human brain activation at high spatial resolution. *Magn. Res. Med.* **29**(1): 139–144.

Fuster, J. M. 1989. *The Prefrontal Cortex. Anatomy, Physiology, and Neuropsychology of the Frontal Lobe.* Raven Press, New York.

George, M. S., Ketter, T. A., and Post, R. M. 1993. SPECT and PET imaging in mood disorders. *J. Clin. Psychiatry* **54:** 6–13.

Gevins, A. S., and Cutillo, B. C. 1993. Neuroelectric evidence for distributed processing in human working memory. *Electroencephalogr. Clin. Neurophysiol.* **87:** 128–143.

Goldman-Rakic, P. S. 1987. Circuitry of primate prefrontal cortex and regulation of behavior by representational memory. In *Handbook of Physiology—The Nervous System,* pp. 373–417.

Goldman-Rakic, P. S. 1991. Prefrontal cortical dysfunction in schizophrenia: The relevance of working memory. In *Psychopathology and the Brain* (B. J. Carroll and J. E. Barrett, Eds.), pp. 1–24. Raven Press, New York.

Harvey, N. 1987. Neurological factors in obsessive compulsive disorder. *Brit. J. Psychiatry* **150:** 567–568.

Hertz-Pannier, L., Galliard, W. D., Mott, S., Cuenod, C. A., Bookheimer S., Weinstein, S., Conry, J., Theodore, W. H., and Le Bihan, D. 1994. Preopperative assessment of language lateralization by fMRI in children with complex partial seizures: Preliminary study. In *Proceedings of the Society of Magnetic Resonance.*

Huttenlocher, P. R. 1979. Synaptic density in human frontal cortex–developmental changes and effects aging. *Brain Res. Amsterdam* **163:** 195—205.

Huttenlocher, P. R., De Courten, C., Garey, L. J., and Van Der Loos, H. 1982. Synaptogenesis in human visual cortex—Evidence for synapse elimination during normal development. *Neurosci. Lett.* **33:** 247–252.

Kennedy, C., and Sokoloff, L. 1957. An adaptation of the nitrous oxide method to the study of the cerebral circulation in children: Normal values for cerebral blood flow and cerebral metabolic rate in childhood. *J. Clin. Invest.* **36:** 1130–1137.

Kim, S. G., Ashe, J., Hendrich, K., Ellermann, J. M., Merkle, H., Ugurbil, K., and Georgopoulos, A. P. 1993. Functional magnetic resonance imaging of motor cortex: Hemispheric asymmetry and handedness. *Science* **261:** 615–617.

Kwong, K. K., Belliveau, J. W., Chesler, D. A., Goldberg, I. E., Weisskoff, R. M., Poncelet, B. P., Kennedy, D. N., Hoppel, B. E., Cohen, M. S., Turner, R., Cheng, H.-M., Brady, T. J., and Rosen, B. R. 1992. Dynamic magnetic resonance imaging of human brain activity during primary sensory stimulation. *Proc. Natl. Acad. Sci. USA* **89:** 5675.

Menon, R. S., Ogawa, S., Tank, D. W., and Ugurbil, K. 1993. 4 Tesla gradient recalled echo characteristics of photic stimulation-induced signal changes in the human primary visual cortex. *Magn. Res. Med.* **30:** 380–386.

Mesalum, M. M. 1985. *Principles of Behavioral Neurology.* Davis, Philadelphia, PA.

Ogawa,S., Lee, T. S., Nayak, A. S., and Glynn, P. 1990. Oxygenation-sensitive contrast in magnetic resonance image of rodent brain at high magnetic fields. *Magn. Res. Med.* **26:** 68–78.

Paulesu, E., Frith, C. D., and Frackowiak, R. S. J. 1993. The neural correlates of the verbal component of working memory. *Nature* **362:** 342–345.

Pascal-Leone, J. A. 1970. A mathematical model for transition in Piaget's developmental stages. *Psychologica* **32:** 301–345.

Raichle, M. E. 1988. Circulatory and metabolic correlates of brain function in normal humans. In *Handbook of Physiology The Nervous System V* (V. B. Mountcastle, F. Plum, and S. R. Geiger, Eds.). American Physiological Society, Bethesda, MD.

Schneider, W., Noll, D. C., and Cohen, J. D. 1993. Functional topographic mapping of the cortical ribbon in human vision with conventional MRI scanners. *Nature* **365:** 150–153.

Schneider, W., Casey, B. J., and Noll, D. C. 1994. Functional MRI mapping of stimulus rate effects across visual processing stages. *Hum. Brain Mapping* **1:** 117–133.

Snedecor, G. W., and Cochran, W. G. 1980. Uses of the correlational coefficient. In *Statistical Methods* (G. W. Snedecor and W. G. Cochran, Eds.), Seventh ed. Iowa State Univ. Press, Ames, Iowa.

Swedo, S., Pietrini, P., Leonard, H. L., Schapiro, M. B., Rettew, D. C., Goldberger, E. L., Rapoport, S. I., Rapoport, J. L., and Grady, C. L. 1989. Cerebral glucose metabolism in Child-Onset Obsessive—Compulsive Disorder. *Arch. Gen. Psychiatry* **49:** 690–694.

Talairach, J., and Tournoux, P. 1988. *Co-planar Stereotaxic Atlas of the Human Brain.* Thieme, New York.

Trommer, B. L., Hoeppner, J. A., and Zecker, S. G. 1991. The go–no-go test in attention deficit disorder is sensitive to methylphenidate. *J. Child Neurol.* **6:** 128–131.

Turner, R., Le Bihan, D., Moonen, C. T. W., Despres, D., and Frank, J. 1991. Echo-planar time course MRI of cat brain oxygenation changes. *Magn. Res. Med.* **22:** 159–166.

Woods, R. *et al.* 1992. *J. Computer Assisted Tomogr.* **16:** 620–633.